

**Biomaterials-Based Strategies for Salivary Gland Tissue  
Regeneration**

Journal:	<i>Biomaterials Science</i>
Manuscript ID	BM-MRV-09-2015-000358.R2
Article Type:	Minireview
Date Submitted by the Author:	26-Dec-2015
Complete List of Authors:	Ozdemir, Tugba; University of Delaware, Materials Science and Engineering Fowler, Eric; University of Delaware, Materials Science and Engineering Hao, Ying; University of Delaware, Materials Science and Engineering Ravikrishnan, Anitha; University of Delaware, Materials Science and Engineering Harrington, Daniel; Rice University, BioSciences and Bioengineering Witt, Robert; Christiana Care Health Systems, Helen F. Graham Cancer Center Farach-Carson, Mary; Rice University, Biochemistry and Cell Biology Pradhan-Bhatt, Swati; Christiana Care Health Systems, Helen F. Graham Cancer Center Jia, Xinqiao; University of Delaware, Materials Science and Engineering

## Biomaterials-Based Strategies for Salivary Gland Tissue Regeneration

Tugba Ozdemir,<sup>1</sup> Eric W. Fowler,<sup>1</sup> Ying Hao,<sup>1</sup> Anitha Ravikrishan,<sup>1</sup> Daniel A. Harrington,<sup>2</sup> Robert L. Witt,<sup>3,4</sup> Mary C Farach-Carson,<sup>2,3</sup> Swati Pradhan-Bhatt,<sup>3,4,5\*</sup> Xinqiao Jia<sup>1,3,5\*</sup>

<sup>1</sup>Department of Materials Science and Engineering, University of Delaware, Newark, DE 19716, USA

<sup>2</sup>Departments of BioSciences and Bioengineering, Rice University, Houston, TX 77251, USA

<sup>3</sup>Department of Biological Sciences, University of Delaware, Newark, DE, 19716, USA

<sup>4</sup>Helen F. Graham Cancer Center and Research Institute, Christiana Care Health Systems, Newark, DE, 19713, USA

<sup>5</sup>Biomedical Engineering Program, University of Delaware, Newark, DE 19716, USA

\*To whom correspondence should be addressed:

Swati Pradhan-Bhatt, Center For Translational Cancer Research, Helen F. Graham Cancer Center & Research Institute, Christiana Care Health Systems, Newark, DE, 19713, USA, Phone: 302-623-4649, Fax: 302-623-4314, Email: [swati@udel.edu](mailto:swati@udel.edu)

Xinqiao Jia, Department of Materials Science and Engineering, University of Delaware, Newark, DE, 19716, USA. Phone: 302-831-6553, Fax: 302-831-4545, E-mail: [xjia@udel.edu](mailto:xjia@udel.edu).

**Keywords:** Epithelial, Salivary Gland, Dry Mouth, Biomaterials, Tissue Engineering, Hydrogels, Fibrous Scaffolds, Assembly, Polarization, Branching.

1 **ABSTRACT.** The salivary gland is a complex, secretory tissue that produces saliva and  
2 maintains oral homeostasis. Radiation induced salivary gland atrophy, manifested as “dry  
3 mouth” or xerostomia, poses a significant clinical challenge. Tissue engineering recently has  
4 emerged as an alternative, long-term treatment strategy for xerostomia. In this review, we  
5 summarize recent efforts towards the development of functional and implantable salivary glands  
6 utilizing designed polymeric substrates or synthetic matrices/scaffolds. Although the *in vitro*  
7 engineering of a complex implantable salivary gland is technically challenging, opportunities  
8 exist for multidisciplinary teams to harvest the regenerative potential of stem/progenitor cells  
9 found in the adult glands and combine them with biomimetic and cell-instructive materials to  
10 assemble implantable tissue modules.

1

2 **1. Introduction.**

3 Salivary glands, including the parotid, submandibular, and sublingual glands as well as  
4 numerous minor glands, produce saliva in response to a wide range of biochemical input and  
5 environmental cues. Control of response is achieved through the cooperative actions of various  
6 cell types that are organized into a complex branched acinar and ductal structure.<sup>1, 2</sup> Located in  
7 the upper aerodigestive tract, the salivary gland can be damaged by radiation therapy for head  
8 and neck cancers, and the patients' quality of life can be severely compromised owing to the  
9 reduced saliva production and altered saliva composition. Manifested as "dry mouth syndrome",  
10 or xerostomia, patients suffer from oral dryness, have difficulty speaking, swallowing, and can  
11 develop dental caries and periodontal diseases. Current treatments for xerostomia temporarily  
12 mitigate the symptoms, but do not provide long-term therapeutic benefits.<sup>3</sup>

13 In 2000, Baum and colleagues proposed the concept of producing an artificial, tissue-  
14 engineered salivary gland as a potential clinical solution for the restoration of salivary function.  
15 Their initial report highlighted the importance of presenting appropriate matrix proteins on  
16 porous polyester scaffolds for the attachment and growth of a human salivary gland-derived cell  
17 line.<sup>4</sup> Our collaborative team further refined the conditions and procedures for salivary gland  
18 tissue engineering using primary human salivary gland epithelial cell populations isolated from  
19 patients undergoing head and neck surgery pre-radiation. The isolated cells are cultured *in vitro*  
20 in synthetic matrices to stimulate cellular organization and tissue growth. Ultimately, the  
21 engineered construct containing integrated structural components will be implanted to the site of  
22 radiation injury for tissue regeneration purposes.<sup>5</sup> Such an autologous cell-based, reverse  
23 engineering approach for salivary gland restoration is challenging, as the tissue development  
24 and maturation depends on the reciprocal interactions between various types of cells and  
25 tissues comprising and surrounding the gland to promote cell survival, proliferation, apoptosis,  
26 adhesion, motility and morphological changes. *Ex vivo* culture of mouse embryonic

1 submandibular gland tissues has revealed key insights in developmental biology,<sup>6-8</sup> that can  
2 inform and direct biomaterials-based approaches for reconstitution of salivary gland architecture  
3 and function. The inaccessibility of human embryonic tissues/cells and their tumorigenic  
4 transformation upon implantation limit their usage in salivary gland tissue engineering.<sup>9</sup>  
5 Therapeutic salivary gland regeneration is possible if adult progenitor cells can be harvested  
6 and reprogrammed to maximize their regenerative capacity.<sup>6</sup>

7 Although cell-cell interactions dictate the assembly of epithelial tissues, the extracellular  
8 matrix (ECM), whether in the form of the basement membrane in direct contact with the  
9 structural units or as a three-dimensional (3D) mesenchyme surrounding the organized salivary  
10 gland tissue, provides biophysical, biomechanical and biochemical cues to guide the epithelial  
11 cells into organized structures and functional tissues.<sup>10, 11</sup> Biomaterials designed for tissue  
12 engineering applications must be biocompatible, biodegradable, biologically relevant and exhibit  
13 tissue-like viscoelasticity. For the *ex vivo* culture of cells of epithelial origin, one must consider  
14 the potential of synthetic matrices to foster cell-cell contact/communication, guide cellular  
15 assembly, direct polarization and induce branching.<sup>12</sup>

16 In this mini review, we first outline the basic structure of the human salivary gland. We then  
17 provide examples of biologically inspired material designs applied to salivary gland tissue  
18 engineering. These are presented in the context of 2D and 3D culture of adult salivary gland  
19 cells, as well as *ex vivo* culture of embryonic tissues. We discuss how properties of materials  
20 affect cellular functions and how materials-derived models can be exploited to gain  
21 understanding of tissue morphogenesis. Salivary gland tissue engineering is still in infancy and  
22 many technical and regulatory challenges remain before an implantable tissue analog can be  
23 translated into the clinic. Nevertheless, it is our belief that the design of tunable, dynamic and  
24 cell-instructive matrices with environmental cues and ECM-derived motifs will ultimately lead to  
25 the development of a deliverable implant device for patients suffering from xerostomia.

26

## 1 2. Salivary Gland Anatomy and Physiology.

2 The salivary gland achieves its secretory function *via* the coordinated actions of assembled  
3 acinar, ductal, and myoepithelial cells (**Figure 1**). While the acinar cells form functional spherical  
4 acini with a common lumen into which to secrete proteins and liquids, the ductal cells create a  
5 tubular conduit to transport acini-derived saliva into the oral cavity. As the protein-rich salivary  
6 mixture flows through the ductal network, its ionic composition is modified. In their respective  
7 units, the acinar and the ductal cells are linked together by complementary cell junctions, such  
8 as occludin, anchoring and communicating junctions. The cytoskeletal filaments, along with  
9 attached cell-cell and cell-matrix adhesion sites, maintain the structural and mechanical integrity  
10 of the assemblies. The organelles and membrane proteins in these cells segregate  
11 heterogeneously in various locations of the intracellular space such that apical, lateral and basal  
12 surfaces form.<sup>1, 5</sup>

13 The epithelial layer, whether in the acinus or in the duct, overlies a basement membrane  
14 that is ~100 nm thick, mainly composed of collagen IV, laminin, nidogen and the proteoglycan  
15 perlecan/HSPG2. Also present in the basement membrane are proteases and their inhibitors, as  
16 well as growth and regulatory proteins, many being sequestered by the heparan sulfate chains  
17 of perlecan. The epithelial cells are attached to the basement membrane through integrin  
18 heterodimers located at the basal membrane of the cells. In a polarized epithelial cell, the basal  
19 membrane contains neurotransmitter receptors and some ion channels, while the junctional  
20 complexes containing E-cadherin and zonula occludens are found near the apex of the lateral  
21 membrane. The apical membrane contains aquaporins and mucins. Myoepithelial cells wrap  
22 around the acini inside the basement membrane that separates them from the surrounding  
23 stroma, purportedly expelling primary saliva from the acini through actomyosin-mediated  
24 contraction.<sup>13</sup> The tight regulation of ECM composition and cell-cell interactions maintain a  
25 polarized structure with a directional secretory function.<sup>10</sup>

1 During development, the salivary gland epithelium undergoes programmed expansion and  
2 morphogenesis to form a complex tissue architecture with branched, interconnected and well-  
3 ordered lobules and ducts. Such morphological transformation requires intimate epithelial-  
4 mesenchymal crosstalk via frequent cycles of cleft formation and bud outgrowth, effectively  
5 maximizing surface area needed to provide sufficient trans-epithelial fluid secretion. The  
6 complex glandular structures bounded by the basement membrane are surrounded by stromal  
7 tissues and are innervated by the peripheral nervous system, which controls saliva production  
8 through sympathetic and parasympathetic mechanisms.<sup>11, 14</sup>

9

### 10 **3. Biomaterials Strategy.**

11 Biomaterials-based tissue engineering strategies for the restoration of salivary gland  
12 function can be generally divided into three categories (**Figure 2, Table 1**). In the first approach  
13 (2D culture, **Figure 2A**),<sup>4</sup> salivary gland cells or cell lines are introduced and cultured as a  
14 monolayer lining a blind-end tubular device of porous and biodegradable polymers. The goal is  
15 to create a polarized epithelial cell monolayer capable of unidirectional fluid secretion. Other 2D  
16 culture studies aim at promoting acinar cell phenotype, expanding the desired cell population or  
17 generating 3D aggregates on 2D surfaces. In the second approach (3D culture, **Figure 2B**),<sup>15</sup>  
18 selected progenitor and epithelial cell populations from dispersed salivary gland cells are  
19 encapsulated in 3D hydrogel matrices, frequently constructed employing bioorthogonal  
20 chemistries (**Figure 3**), and allowed to proliferate and assemble. 3D assembly can reconstitute  
21 the polarized and secretory acinar structures that are envisioned to connect and integrate with  
22 the existing ductal structure in the lack –secretory uncer, availability of expanded progenitor cell  
23 populations from adult human tissues with inherent acinar assembly capacity, secretory  
24 functions and regenerative potential. In the third approach (*ex vivo* culture of embryonic tissues,  
25 **Figure 2C**),<sup>16</sup> embryonic salivary gland tissues or cells are cultured on a compliant substrate to  
26 allow for branching morphogenesis to occur *in vitro*. These studies have revealed key insights

1 into the developmental biology of the salivary gland, providing guidance in the design of  
2 effective therapies for the repair of damaged glands and the regeneration of functional  
3 substitutes.

4  
5 **3.1. 2D Culture.** The original design of an artificial salivary gland<sup>17</sup> requires a secretory  
6 device containing a cohesive monolayer of ductal cells lining the interior of a tube fabricated  
7 from commercial polymers that not only promote cell attachment and growth, but also preserve  
8 the desired cell phenotype. Yamada and Baum investigated the suitability of biodegradable  
9 polyesters (PLA: poly(lactic acid), PGA: poly(glycolic acid)) for the growth and organization of a  
10 human salivary ductal epithelial cell line (HSG). In general, substrates without any ECM coating  
11 do not support robust cell attachment and growth. Substrates coated with proteins derived from  
12 basement membrane (Matrigel®, laminin, or collagen IV) foster the slow growth of adherent  
13 cells and facilitate the development of organized 2D cell aggregates. Substrates coated with  
14 proteins more characteristic of interstitial tissue (collagen I or fibronectin) promote the rapid  
15 development of HSG cell monolayers.<sup>4</sup> However, the inability of HSG cells to form a polarized  
16 monolayer and to establish tight junctions, combined with their potential to undergo malignant  
17 transformation *in vivo*, prohibited the widespread usage of these cells for salivary gland tissue  
18 engineering purposes.<sup>9, 18</sup>

19 As researchers continue to identify and isolate human cells for salivary gland tissue  
20 engineering, parallel effort has been focused on the development of appropriate biomaterial  
21 scaffolds to support the proliferation and differentiation of salivary gland progenitors. Porous  
22 membranes or scaffolds of relatively hydrophobic polymers, such as poly(vinylidene fluoride)  
23 (PVDF) or silk fibroin, are more supportive of cell growth<sup>19</sup> and phenotype retention<sup>20</sup> than flat  
24 substrates. Fibronectin-coated silk fibroin scaffolds supported the development of aggregates  
25 that resemble the secretory acini morphologically and functionally. Cells cultured under these  
26 conditions maintained their differentiated secretory function for approximately one month. These



1 materials can be used for growing and expanding highly differentiated salivary gland cells for  
2 salivary gland regeneration purposes. Therefore, a tubular scaffold with dense outer surface to  
3 prevent saliva leakage and a porous inner surface for the cell attachment and growth can be  
4 utilized for the creation of an artificial salivary gland.

5 Under appropriate conditions, monolayer culture on flat surfaces also can give rise to  
6 multicellular spherical structures, expressing acinar-like phenotype. Our group conducted a pilot  
7 study by culturing primary human salivary gland cells on photocrosslinked hyaluronic acid (HA)  
8 hydrogels incorporating an 18-amino acid long peptide, identified from the domain IV of  
9 perlecan (PInDIV) and known to support cell adhesion, spreading and FAK activation.<sup>21, 22</sup> Self-  
10 assembly of acini-like structures with tight junctions,  $\alpha$ -amylase expression and an apoptotic  
11 central lumen was observed among structures formed on these HA-based gels.<sup>23</sup> Separately,  
12 primary human parotid gland acinar cells spontaneously formed 3D cell aggregations after  
13 reaching confluence on tissue culture polystyrene (TCPS), and more frequently, on poly (lactic-  
14 co-glycolic acid) (PLGA). However, these post-confluence 3D structures are fairly disorganized,  
15 potentially because of the absence of basement membrane signals.<sup>17</sup>

16 In a comparative study, human parotid and submandibular gland cells were plated onto  
17 either Matrigel®-coated or uncoated TCPS. On uncoated plastic surfaces, monolayers of ductal  
18 cells with tight junctions were observed. On Matrigel®-coated substrates, cells formed 3D  
19 acinar-like units, adopted an acinar phenotype with many secretory granules, and expressed  $\alpha$ -  
20 amylase and the water channel protein, aquaporin-5 (AQP5).<sup>24</sup> Work from our group shows that  
21 coating of TCPS with PInDIV peptide or Matrigel® elicited the same cellular responses from  
22 primary human salivary gland cells, and both coatings support the formation of 3D acini-like  
23 salivary units that express  $\alpha$ -amylase. The synthetic nature of PInDIV peptide enables the  
24 culture of human acinar cells free of animal products, thus representing a step forward towards  
25 the creation of implantable artificial gland.<sup>22</sup>

1 Owing to the structural similarities to the basement membrane, fibrous polymer scaffolds,<sup>25</sup>  
2 most often produced by electrospinning, have been used to culture salivary gland epithelial  
3 cells. In an exploratory study, Larson and co-workers<sup>26</sup> investigated the effects of topography on  
4 behaviors of immortalized adult mouse or rat salivary gland cell lines (SIMS, ductal; Par-C10,  
5 acinar). Compared to cells grown on planar surfaces of the same composition, cells cultured on  
6 the fibrous scaffolds exhibited a more rounded and clustered morphology, as well as a reduced  
7 and more diffuse expression of focal adhesion proteins. A follow-up study<sup>27</sup> revealed that cell  
8 proliferation and polarization strongly depend on the surface coating of the nanofiber scaffolds.  
9 While chitosan coating promoted cell proliferation, appropriate polarization and mature tight  
10 junctions were observed only when the scaffold was coated with laminin-111. Bifunctional  
11 scaffolds containing chitosan and laminin-111 signals induced responses from both acinar and  
12 ductal cell lines.

13 To further mimic the architecture of the basement membrane surrounding spherical acini of  
14 salivary gland epithelial cells, Soccia<sup>28</sup> created ordered arrays of "craters" in  
15 polydimethylsiloxane (PDMS) and lined them with electrospun poly(lactic acid-co-glycolic acid)  
16 (PLGA) nanofibers (**Figure 4E**). Using SIMS and Par-C10 cells, the authors found that  
17 increasing crater curvature increased the average height of the SIMS cell monolayer, cell  
18 polarization, cellular expression (both SIMS and Par-C10 cells) of AQP5 and tight junction  
19 protein occludin in Par-C10 cells. This work highlights the potential of physical features,  
20 including surface chemistry and scaffold stiffness, to promote differentiation of salivary gland  
21 cells.

22 Although processing polymers into fibrous scaffolds by electrospinning is straightforward,  
23 the direct incorporation of biological motifs during electrospinning is more complicated.  
24 Moreover, the physical and mechanical properties of the fibrous scaffolds cannot be tuned  
25 easily using the same polymer. Work from the Fox and Jia laboratories has demonstrated the  
26 utility of tetrazine (Tz) ligation with *trans*-cyclooctenes (TCO), a highly efficient, bioorthogonal

1 reaction<sup>29, 30</sup> (**Figure 3D**) that proceeds with exceptional rates without any catalysis, for the *de*  
2 *novo* synthesis of multiblock copolymer fibers (**Figure 4F, G**).<sup>31</sup> Using a hydrophilic  
3 poly(ethylene glycol) (PEG)-based tetrazine monomer and an aliphatic TCO monomer with a  
4 dodecyl (C12) linker, the polymerization can be carried out at the immiscible water/oil interface.  
5 As the polymerization proceeded, mechanically robust polymer fibers (9-10  $\mu\text{m}$  in diameter) with  
6 molecular weight up to 263 kDa were continuously pulled out of the interface. The bioorthogonal  
7 nature of the tetrazine ligation permits facile incorporation of functional peptides into the  
8 multiblock constructs. When a fibronectin-based peptidic building block (GRGDSP) was  
9 included in the monomer mixture, interfacial bioorthogonal polymerization produced  
10 mechanically robust cell-adhesive microfibers. Human salivary gland myoepithelial cells  
11 attached to the RGD fibers, developed long and narrow lamellipodia and oriented parallel to the  
12 long axis of the fiber. In some cases, multiple cells formed a cohesive blanket enclosing the  
13 fiber.<sup>31</sup> Overall, the peptide-containing fibers present appropriate biochemical signals and  
14 topographical features for the anchorage and alignment of myoepithelial-like cells that may  
15 facilitate assembly of fully functional salivary gland tissues.

16

17 **3.2. 3D culture.** Isolated salivary gland cells traditionally are cultured in hydrogels derived  
18 from natural proteins extracted from animal tissues, such as Matrigel®,<sup>32</sup> collagen gel,<sup>33</sup> and  
19 fibrin gel,<sup>34</sup> or a mixture of fibrin gel and collagen gel.<sup>35</sup> In these hydrogel systems, dispersed  
20 salivary gland cells divide and assemble into 3D acinar-like and/or ductal-like structures, where,  
21 depending on phenotype, they express subsets of tight junction proteins, such as ZO-1,  
22 occludin, and claudin-1, and a critical water channel protein, AQP5. Additional growth and  
23 differentiation factors are necessary to create and maintain the differentiated phenotype, to  
24 stabilize the basic functional units and to induce branching.<sup>32-34</sup> To more fully recapitulate the  
25 native salivary gland microenvironment, decellularized submandibular glands were used as  
26 scaffolds for the 3D culture of rat submandibular gland cells. Cells seeded into the scaffold via

1 injection through the main gland duct and cultured under rotational conditions, adhered to the  
2 scaffold, expressed the differentiated markers, and formed gland-like tissues.<sup>36</sup>

3 While generally conducive to cell assembly, migration and organization, reconstituted  
4 biomaterials derived from natural tissues lack the tunability and reproducibility seen in synthetic  
5 matrices and are potentially tumorigenic or immunogenic. Thus, there is a critical need to  
6 develop synthetic matrices or scaffolds that recreate the developmental niches and exhibit  
7 tunable properties and cell-instructive signals for the establishment of functional and clinically  
8 translatable products to relieve xerostomia. To date, synthetic hydrogels utilized for salivary  
9 gland tissue engineering purposes are based largely on PEG and HA.<sup>15, 37, 38</sup> Synthesized by  
10 living ring-opening polymerization,<sup>39</sup> mono-disperse PEG with controlled molecular weight and  
11 defined end groups are commercially available.<sup>40</sup> Shubin et al. evaluated the suitability of PEG-  
12 based hydrogels, crosslinked by radical chain polymerization (**Figure 3A**) or thiol-ene  
13 polymerization (**Figure 3B1**), for the 3D culture of primary mouse submandibular gland (SMG)  
14 cells, a mixture of acinar and ductal cells. Although the thiol-ene network was found to be more  
15 cytocompatible than the radically crosslinked counterpart, the SMG cells entrapped at single cell  
16 state in both types of gels failed to form organized structures. Encapsulation of pre-assembled  
17 multicellular spheroids improved cell viability, promoted cell proliferation, and established and  
18 preserved cell-cell contacts.<sup>41</sup>

19 Although not present in the basement membrane of the epithelium, HA is a ubiquitous, non-  
20 sulfated glycosaminoglycan (GAG) found in the surrounding mesenchyme, and is especially  
21 abundant in early embryos. Unlike PEG, HA is biologically active, binding specific cell surface  
22 receptors and directing multiple cell functions including adhesion, migration, and  
23 morphogenesis.<sup>42</sup> High molecular weight (1-2 MDa) HA is produced by bacterial fermentation.  
24 Subsequent degradation of the high molecular weight HA by chemical or enzymatic means  
25 results in medium or low molecular weight fragments.<sup>38</sup> Our group has synthesized HA  
26 derivatives bearing mutually reactive functional groups that participate in Michael addition

1 **(Figure 3B2)**<sup>43</sup> or hydrazone ligation **(Figure 3C)**<sup>44, 45</sup> to initiate fast, biocompatible gelation in  
2 bulk for the fabrication of cell-laden gel constructs.<sup>46, 47</sup>

3 Our collaborative team is investigating the utility of these synthetic matrices for salivary  
4 gland tissue engineering purposes. Pradhan et al. developed methods for isolating salivary  
5 gland acinar-like cell populations from tissue specimens harvested from patients undergoing  
6 head and neck surgery.<sup>22</sup> Primary human salivary gland cells were encapsulated in an HA  
7 hydrogel with an elastic modulus of 60-100 Pa.<sup>15</sup> Overtime, cells self-assembled into organized  
8 acini-like structures ~50  $\mu\text{m}$  in size **(Figure 5)**. Additionally, neurotransmitter stimulation of these  
9 acini-like structures via  $\beta$ -adrenergic agonists led to increased granule and  $\alpha$ -amylase  
10 production. Cholinergic stimulation led to intracellular calcium release with oscillations within  
11 these structures, indicative of an active fluid production pathway. Encapsulated cells in 3D  
12 retained their spheroid structure and structural integrity, along with the salivary biomarkers and  
13 maintained viability for over three weeks *in vivo* in an athymic rat model.<sup>37</sup> As discussed above,  
14 the inclusion of PlnDIV peptide in 2D cultures on HA gels stimulates the formation of polarized  
15 acinus with a hollow lumen.<sup>23</sup> We have synthesized macromolecular version of PlnDIV  
16 (MacroPlnDIV) by adopting our established polymerization and conjugation protocols<sup>48-50</sup> to  
17 present multiple repeats of the peptide signals along the polymer backbone similar to those in  
18 native perlecan domain IV. Our ongoing effort is dedicated to the incorporation of MacroPlnDIV  
19 in HA hydrogels to elicit the desired cell assembly/polarization via potent and coordinated cell-  
20 matrix interactions.

21 Recently, tetrazine ligation **(Figure 3D)** has been applied to hydrogel synthesis *via* an  
22 interfacial bioorthogonal gelation process using high molecular weight tetrazine-modified HA  
23 (HA-Tz, 218 kDa) and low molecular weight PEG-based TCO crosslinker (bisTCO, 1,253 Da).  
24 Because the crosslinking is diffusion controlled, hydrogel spheres with 3D spatial patterns  
25 **(Figure 4A)** and water-filled hydrogel channels **(Figure 4B)** can be fabricated readily without

1 the need for external templates or stimuli.<sup>51</sup> These bioorthogonal hydrogel platforms are being  
2 explored for the *in vitro* assembly of secretory acini with interconnected ducts.

3 In addition to immobilized peptide signals, soluble growth factors presented in the hydrogel  
4 matrix in a spatio/temporal manner are indispensable to generate interconnected and branched  
5 salivary gland structures. Other growth factors initiate innervation and angiogenesis needed for  
6 host integration. We have synthesized stably crosslinked, nanoporous HA-based hydrogel  
7 particles (HGPs, **Figure 4C**) by inverse emulsion polymerization.<sup>52, 53</sup> HGPs decorated with  
8 perlecan domain I (PInDI)<sup>54</sup> or heparin<sup>55</sup> sequester heparin binding growth factors and control  
9 their release. Doubly crosslinked networks (**Figure 4D**) have been created using HA HGPs as  
10 the structural units, cell attachment points and growth factor depots to promote desired cellular  
11 responses necessary for the regeneration of functional neotissues.<sup>43, 56-58</sup>

12

13 **3.3. Ex Vivo Culture.** The third strategy for salivary gland regeneration relies on the intrinsic  
14 power of embryonic tissues to undergo programmed branching morphogenesis for the creation  
15 of replacement tissue by *ex vivo* culture of embryonic salivary glands.<sup>59</sup> Further, *ex vivo* organ  
16 culture using mouse embryonic glands has shed critical insight on salivary gland development.  
17 <sup>8, 11, 14</sup> Key features of the expanding embryonic tissue include: (1) a distensible basement  
18 membrane that undergoes dynamic remodeling by proteolytic degradation;<sup>60</sup> (2) an enhanced  
19 motility of the outer epithelial bud cells mediated through integrin-dependent cell-matrix  
20 association;<sup>61</sup> (3) a mechanochemical checkpoint for cleft initiation/progression;<sup>62</sup> and (4) a  
21 deposition of fibronectin in the cleft regions that facilitates and stabilized cleft formation.<sup>63</sup>

22 The regenerative potential of the embryonic tissue is striking; even dissociated epithelial  
23 cells can self-organize and undergo branching morphogenesis to form tissues with structural  
24 features and differentiation markers characteristic of the intact gland.<sup>64</sup> Recently, Ogawa et al.<sup>65</sup>  
25 demonstrated the full functional regeneration of a salivary gland through the orthotopic  
26 transplantation of a bioengineered salivary gland germ, reconstituted with epithelial and

1 mesenchymal single cells isolated from the mouse gland germ at embryonic day 13.5–14.5. The  
2 bioengineered germ develops into a mature, innervated gland with functional acini, capable  
3 secreting salivary fluid that can protect against oral bacterial infections and can effectively  
4 restore normal swallowing in a salivary gland-defective mouse model. Although this study  
5 provides a proof-of-concept bioengineering approach for the treatment xerostomia, the lack of  
6 human embryonic tissues prohibits widespread application of such a strategy for patients with  
7 xerostomia.

8 Available biomaterials that support branching morphogenesis of embryonic salivary glands  
9 include PVDF,<sup>66</sup> chitosan,<sup>67, 68</sup> alginate gel,<sup>69</sup> fibrous PLGA scaffold,<sup>26</sup> and polyacrylamide gel.<sup>16</sup>  
10 For alginate and polyacrylamide gels, surface conjugation with a cell adhesive peptide (RGD) or  
11 fibronectin is necessary to improve cell/tissue adhesion. Not surprisingly, substrate stiffness  
12 affects branching morphogenesis.<sup>69, 70</sup> In general, softer gels (alginate<sup>69</sup> or polyacrylamide,<sup>16</sup>)  
13 enhance bud expansion and cleft formation, whereas stiffer gels attenuate them (**Figure 6**).  
14 Glands cultured on soft gels (4 kPa for alginate gels, and 0.48 kPa for polyacrylamide gels)  
15 better resemble developing glands both morphologically and phenotypically, assessed by  
16 expression of differentiation markers reflecting various cells in the gland. On stiff gels (184 kPa  
17 for alginate gels and 20 kPa for polyacrylamide gels), however, tissue morphology, as well as  
18 the expression and distribution of smooth muscle  $\alpha$ -actin and AQP5 were altered. Transfer of  
19 glands from stiff to soft gels or the addition of exogenous growth factors, such as fibroblast  
20 growth factors (FGF 7/10) or transforming growth factor  $\beta$ 1 (TGF- $\beta$ 1), resulted in substantial  
21 recovery or partial rescue of acinar structure and differentiation. These results indicate that  
22 mechanical environments, in addition to chemical signals, should be modeled to better promote  
23 organ development in the contexts of salivary gland tissue engineering.

24

#### 25 **4. Strategies, Challenges and Future Directions**

1 Challenges lie ahead for each approach to the *in vitro* production of a prototype replacement  
2 salivary gland (**Figure 2**). In the first envisioned approach that relies on a blind-end tube and a  
3 monolayer of duct cells, scaffolds with porous/fibrous features and immobilized basement  
4 membrane signals on the luminal surface are conducive to growth of a cohesive cell monolayer  
5 with intimate cell-cell junctions. The inability of non-secretory ductal cells to secrete proteins and  
6 fluids into the lumen of the tubular device, combined with the adverse tissue responses to the  
7 implanted scaffolds, posed a significant challenge for the clinical translation of such a device.  
8 Gene transfer of cDNAs encoding various water channel proteins and secretory proteins is  
9 being exploited to install the secretory functions in ductal cells.<sup>9, 71</sup> To date, it is not clear how to  
10 stably and efficiently transfer multiple genes to isolated ductal cells. The safety concerns over  
11 the usage of viral vectors and genetically manipulated cells add another level of complexity.  
12 Moreover, studies have shown that the implantation of cell-free tubular PLA or PLGA devices  
13 elicited moderate inflammation and adverse wound healing responses that may destroy the  
14 lining salivary gland cells or plug the open ends. The breakdown of both the polymeric scaffolds  
15 adjacent to the oral mucosa, along with the potential for associated damage to the lining graft  
16 cells, could provide a source for local mucosal immune challenge.<sup>72</sup> Owing to these  
17 complications and the lack of validation data, this strategy that relies on the reengineering of  
18 ductal cells for the creation of a secretory device has largely been abandoned.

19 The second approach aims at establishing a functional secretory construct using isolated  
20 acinar (or acinar-like) cells and bioactive scaffolds. Obviously, both mechanical and  
21 chemical/biochemical parameters affect cell assembly and organogenesis.<sup>69, 73, 74</sup> Unfortunately,  
22 synthetic matrices that foster selective differentiation and organization of multiple cell types  
23 have not yet been developed. At a more fundamental level with regard to the hydrogel design,  
24 several materials parameters must be considered. When dispersed as single cells during the  
25 initial gelation process, salivary gland epithelial cells do not assemble into organized acinar-like  
26 structures in stably and densely crosslinked hydrogels as they cannot proliferate and migrate



1 towards each other in such networks.<sup>41</sup> Additionally, healthy adult salivary epithelial cells do not  
2 actively engage in the remodeling of their surrounding stroma environment.<sup>75-77</sup> A more  
3 permissive network structure can be generated by tuning the crosslinker length, the linker  
4 chemistry, the degree of crosslinking and the network connectivity. Non-covalent interactions<sup>78</sup>  
5 or reversible covalent bonds<sup>79, 80</sup> can be introduced to impart dynamic properties to the matrices  
6 without compromising the network integrity. A programmed introduction of various biological  
7 signals, in a multivalent fashion,<sup>81, 82</sup> can promote the desired cellular functions at different  
8 stages of tissue assembly.<sup>83</sup>

9 An alternate strategy for salivary gland tissue engineering is to create well-defined 3D acinar  
10 spheroids with close and intimate cell-cell contacts using micro-fabricated templates.<sup>84, 85</sup>  
11 Entrapping these pre-formed spheroids in a synthetic matrix along with other types of cells  
12 found in the salivary gland exhibiting matrix remodeling capacity to establish a 3D co-culture  
13 system is an attractive strategy to overcome the network restriction and to foster the functionally  
14 stable co-assembly of tissue structures.<sup>86</sup> As discussed above, fibrous scaffolds mimic the  
15 basement membrane morphologically; however, cells directly plated on the scaffold are  
16 essentially cultured on 2D. One can apply materials fabrication techniques to introduce  
17 macroscopic, interconnected channels or pores within the fibrous scaffolds.<sup>87</sup> Cells residing in  
18 the macropores or channels are surrounded by the fibrous mesh. As the cells assemble and  
19 connect within the scaffold, an integrated 3D construct can be generated and manipulated.<sup>88</sup>

20 If appropriately polarized secretory acini are produced, the next technical hurdle is the  
21 replication of the ordered and highly branched tissue architecture. So far, branching  
22 morphogenesis has been reproduced *in vitro* using embryonic submandibular gland bud,<sup>11, 67</sup>  
23 but not yet reproduced using human salivary gland epithelial cells isolated from adult tissues. To  
24 overcome this technical hurdle, it is tempting, from a materials perspective, to further introduce  
25 more complicated molecular and physical information coded in the native tissue to the synthetic  
26 scaffolds. However, for clinical translation of tissue engineering products, cost-effectiveness,

1 scalability and the ease of production must be considered.<sup>88</sup> In this context, a realistic and  
2 immediate goal is to produce the construct containing numerous secretory acini, that once  
3 implanted, will reconnect to the ducts that are spared by radiation therapy.<sup>1</sup>

4 The third approach harvests the regenerative potential of embryonic tissues. On this front,  
5 biomaterials can be designed with the appropriate stiffness and biological signals to maintain  
6 the appropriate cell phenotypes, to accelerate the branching morphogenesis and to ensure  
7 appropriate spatial organization of multiple cell types in the developing gland. Although the  
8 embryonic stem cells/tissues have a significant potential to generate various tissues, their  
9 application in tissue engineering is restricted owing to ethical and safety concerns. Recent  
10 identification of stem/progenitor cell populations in the adult salivary gland offers opportunities to  
11 generate all cell types present in the gland via programmed differentiation.<sup>89-91</sup> Still, the  
12 establishment of a fully functional gland requires additional methods for isolation, purification  
13 and expansion of other types of supporting cells found in the gland.

14 In all three approaches, the implanted tissue ideally should be vascularized and innervated  
15 by the host tissue so that the neotissue receives sufficient oxygen and nutrients, and the  
16 secretory function can be controlled by an integrated host nervous system. Overall, tissue  
17 engineering of salivary gland is scientifically and technically challenging. More concerted efforts  
18 from investigators with diverse backgrounds are needed to make construction of an engineered  
19 salivary gland a reality.

20

## 21 **5. Conclusions.**

22 In this mini review, we describe the structure and the function of salivary gland and outline  
23 biomaterials-based strategies for salivary gland tissue engineering. We discuss the limitations of  
24 the current materials platforms. Despite these present obstacles, the prospects for tissue  
25 engineering with the use of biomimetic scaffolds offer distinct advantages for long term  
26 functional restoration of salivary glands. Functional neotissue derived from autologous cells

1 seeded in a network of modified scaffolds could be implanted in a patient with potentially  
2 minimal immunogenic risk. Nonetheless, the rate of recent progress is impressive, and there  
3 remains a high likelihood that at least one of these strategies will provide useful new avenues to  
4 generate glandular tissue replacements for patients with xerostomia.

5

6 **Acknowledgements:** Work in the authors' laboratories has been funded by grants from the  
7 National Science Foundation (DMR/BMAT 1206310), National Institutes of Health (R01  
8 DE022969). We acknowledge the Delaware COBRE program (NIGMS: P30 GM110758) for  
9 instrumentation support. The authors wish to acknowledge Genzyme for generously providing  
10 HA. X. J. acknowledges funding support from DuPont (DuPont Young Professor).

11

1

2 **References:**

- 3 1. R. L. Witt, *Salivary gland diseases: surgical and medical management*, Thieme, New  
4 York, 2005.
- 5 2. D. A. Harrington, M. Martinez, D. Wu, S. Pradhan-Bhatt and M. C. Farach-Carson, in  
6 *Advances in Salivary Diagnostics*, ed. C. F. Streckfus, Springer Berlin Heidelberg, 2015,  
7 pp. 157-185.
- 8 3. R. M. Nagler and B. J. Baum, *Archives of otolaryngology--head & neck surgery*, 2003,  
9 **129**, 247-250.
- 10 4. D. J. Aframian, E. Cukierman, J. Nikolovski, D. J. Mooney, K. M. Yamada and B. J.  
11 Baum, *Tissue engineering*, 2000, **6**, 209-216.
- 12 5. S. Pradhan-Bhatt, K. Cannon, D. Zakheim, D. A. Harrington, R. L. Duncan, X. Jia, M. C.  
13 Farach-Carson and R. L. Witt, in *Stem Cell Biology and Tissue Engineering in Dental*  
14 *Sciences*, eds. P. S. Vishwakarma A; Sharpe, S; and M. Ramalingham, Elsevier, 2014,  
15 pp. 613-623.
- 16 6. I. M. Lombaert, S. M. Knox and M. P. Hoffman, *Oral diseases*, 2011, **17**, 445-449.
- 17 7. W. M. Knosp, S. M. Knox and M. P. Hoffman, *Wiley interdisciplinary reviews.*  
18 *Developmental biology*, 2012, **1**, 69-82.
- 19 8. V. N. Patel and M. P. Hoffman, *Seminars in cell & developmental biology*, 2014, **25**, 52-  
20 60.
- 21 9. D. J. Aframian and A. Palmon, *Tissue Eng Part B Rev*, 2008, **14**, 187-198.
- 22 10. B. Alberts, A. Johnson, J. Lewis, M. Raff., K. Roberts and P. Walter, in *Molecular Biology*  
23 *of the Cell*, Garland Science, New York, 4th Ed edn., 2002, pp. 1065-1125.
- 24 11. V. N. Patel, I. T. Rebutini and M. P. Hoffman, *Differentiation; research in biological*  
25 *diversity*, 2006, **74**, 349-364.
- 26 12. N. E. Vrana, P. Lavalley, M. R. Dokmeci, F. Dehghani, A. M. Ghaemmaghami and A.  
27 Khademhosseini, *Tissue Eng Part B Rev*, 2013, **19**, 529-543.
- 28 13. R. T. Chitturi, V. Veeravarmal, R. M. Nirmal and B. V. Reddy, *Journal of clinical and*  
29 *diagnostic research : JCDR*, 2015, **9**, ZE14-18.
- 30 14. J. Harunaga, J. C. Hsu and K. M. Yamada, *Journal of dental research*, 2011, **90**, 1070-  
31 1077.
- 32 15. S. Pradhan-Bhatt, D. A. Harrington, R. L. Duncan, X. Jia, R. L. Witt and M. C. Farach-  
33 Carson, *Tissue engineering. Part A*, 2013, **19**, 1610-1620.
- 34 16. S. B. Peters, N. Naim, D. A. Nelson, A. P. Mosier, N. C. Cady and M. Larsen, *Tissue*  
35 *Eng Part A*, 2014, **20**, 1632-1642.
- 36 17. Y. H. Chan, T. W. Huang, Y. S. Chou, S. H. Hsu, W. F. Su, P. J. Lou and T. H. Young,  
37 *Biomaterials*, 2012, **33**, 464-472.
- 38 18. D. J. Aframian, S. D. Tran, E. Cukierman, K. M. Yamada and B. J. Baum, *Tissue*  
39 *engineering*, 2002, **8**, 871-878.
- 40 19. M. H. Chen, Y. H. Hsu, C. P. Lin, Y. J. Chen and T. H. Young, *Journal of biomedical*  
41 *materials research. Part A*, 2005, **74**, 254-262.
- 42 20. B. X. Zhang, Z. L. Zhang, A. L. Lin, H. Wang, M. Pilia, J. L. Ong, D. D. Dean, X. D. Chen  
43 and C. K. Yeh, *Tissue Eng Part A*, 2015, **21**, 1611-1620.
- 44 21. M. C. Farach-Carson, A. J. Brown, M. Lynam, J. B. Safran and D. D. Carson, *Matrix*  
45 *biology : journal of the International Society for Matrix Biology*, 2008, **27**, 150-160.
- 46 22. S. Pradhan, C. Zhang, X. Jia, D. D. Carson, R. Witt and M. C. Farach-Carson, *Tissue*  
47 *Eng Part A*, 2009, **15**, 3309-3320.

- 1 23. S. Pradhan, C. Liu, C. Zhang, X. Jia, M. C. Farach-Carson and R. L. Witt,  
2 *Otolaryngology--head and neck surgery : official journal of American Academy of*  
3 *Otolaryngology-Head and Neck Surgery*, 2010, **142**, 191-195.
- 4 24. O. M. Maria, A. Zeitouni, O. Gologan and S. D. Tran, *Tissue Eng Part A*, 2011, **17**, 1229-  
5 1238.
- 6 25. D. Liang, B. S. Hsiao and B. Chu, *Advanced drug delivery reviews*, 2007, **59**, 1392-  
7 1412.
- 8 26. S. J. Sequeira, D. A. Soscia, B. Oztan, A. P. Mosier, R. Jean-Gilles, A. Gadre, N. C.  
9 Cady, B. Yener, J. Castracane and M. Larsen, *Biomaterials*, 2012, **33**, 3175-3186.
- 10 27. S. I. Cantara, D. A. Soscia, S. J. Sequeira, R. P. Jean-Gilles, J. Castracane and M.  
11 Larsen, *Biomaterials*, 2012, **33**, 8372-8382.
- 12 28. D. A. Soscia, S. J. Sequeira, R. A. Schramm, K. Jayarathanam, S. I. Cantara, M. Larsen  
13 and J. Castracane, *Biomaterials*, 2013, **34**, 6773-6784.
- 14 29. M. L. Blackman, M. Royzen and J. M. Fox, *J Am Chem Soc*, 2008, **130**, 13518-13519.
- 15 30. M. T. Taylor, M. L. Blackman, O. Dmitrenko and J. M. Fox, *J Am Chem Soc*, 2011, **133**,  
16 9646-9649.
- 17 31. S. Liu, H. Zhang, R. A. Remy, F. Deng, M. E. Mackay, J. M. Fox and X. Jia, *Advanced*  
18 *materials (Deerfield Beach, Fla.)*, 2015, **27**, 2783-2790.
- 19 32. V. Szlavik, J. Vag, K. Marko, K. Demeter, E. Madarasz, I. Olah, T. Zelles, B. C.  
20 O'Connell and G. Varga, *Journal of cellular biochemistry*, 2008, **103**, 284-295.
- 21 33. M. Furue, T. Okamoto, H. Hayashi, J. D. Sato, M. Asashima and S. Saito, *In vitro cellular*  
22 *& developmental biology. Animal*, 1999, **35**, 131-135.
- 23 34. A. D. McCall, J. W. Nelson, N. J. Leigh, M. E. Duffey, P. Lei, S. T. Andreadis and O. J.  
24 Baker, *Tissue Eng Part A*, 2013, **19**, 2215-2225.
- 25 35. A. Joraku, C. A. Sullivan, J. Yoo and A. Atala, *Differentiation; research in biological*  
26 *diversity*, 2007, **75**, 318-324.
- 27 36. Z. Gao, T. Wu, J. Xu, G. Liu, Y. Xie, C. Zhang, J. Wang and S. Wang, *Cells, tissues,*  
28 *organs*, 2014, **200**, 171-180.
- 29 37. S. Pradhan-Bhatt, D. A. Harrington, R. L. Duncan, M. C. Farach-Carson, X. Jia and R. L.  
30 Witt, *Laryngoscope*, 2014, **124**, 456-461.
- 31 38. K. T. Dicker, L. A. Gurski, S. Pradhan-Bhatt, R. L. Witt, M. C. Farach-Carson and X. Jia,  
32 *Acta biomaterialia*, 2014, **10**, 1558-1570.
- 33 39. C. Mangold, F. Wurm and H. Frey, *Polym. Chem.*, 2012, **3**, 1714-1721.
- 34 40. J. Zhu, *Biomaterials*, 2010, **31**, 4639-4656.
- 35 41. A. D. Shubin, T. J. Felong, D. Graunke, C. E. Ovitt and D. S. Benoit, *Tissue Eng Part A*,  
36 2015, **21**, 1733-1751.
- 37 42. H. G. Garg and C. A. Hales, *Chemistry and biology of hyaluronan*, Elsevier Ltd., Oxford,  
38 2004.
- 39 43. X. Xu, L. A. Gurski, C. Zhang, D. A. Harrington, M. C. Farach-Carson and X. Jia,  
40 *Biomaterials*, 2012, **33**, 9049-9060.
- 41 44. L. A. Gurski, A. K. Jha, C. Zhang, X. Jia and M. C. Farach-Carson, *Biomaterials*, 2009,  
42 **30**, 6076-6085.
- 43 45. A. J. Farran, S. S. Teller, A. K. Jha, T. Jiao, R. A. Hule, R. J. Clifton, D. P. Pochan, R. L.  
44 Duncan and X. Jia, *Tissue engineering. Part A*, 2010, **16**, 1247-1261.
- 45 46. X. Xu, A. K. Jha, D. A. Harrington, M. C. Farach-Carson and X. Jia, *Soft matter*, 2012, **8**,  
46 3280-3294.
- 47 47. S. Liu, K. T. Dicker and X. Jia, *Chemical communications (Cambridge, England)*, 2015,  
48 **51**, 5218-5237.
- 49 48. S. E. Grieshaber, A. J. Farran, S. Lin-Gibson, K. L. Kiick and X. Jia, *Macromolecules*,  
50 2009, **42**, 2532-2541.

- 1 49. S. E. Grieshaber, A. J. Farran, S. Bai, K. L. Kiick and X. Jia, *Biomacromolecules*, 2012,  
2 **13**, 1774-1786.
- 3 50. L. Xiao, J. Zhu, D. J. Londono, D. J. Pochan and X. Jia, *Soft matter*, 2012, **8**, 10233-  
4 10237.
- 5 51. H. Zhang, K. T. Dicker, X. Xu, X. Jia and J. M. Fox, *ACS macro letters*, 2014, **3**, 727-  
6 731.
- 7 52. X. Jia, Y. Yeo, R. J. Clifton, T. Jiao, D. S. Kohane, J. B. Kobler, S. M. Zeitels and R.  
8 Langer, *Biomacromolecules*, 2006, **7**, 3336-3344.
- 9 53. N. Sahiner, A. K. Jha, D. Nguyen and X. Jia, *Journal of biomaterials science. Polymer*  
10 *edition*, 2008, **19**, 223-243.
- 11 54. A. K. Jha, W. Yang, C. B. Kirn-Safran, M. C. Farach-Carson and X. Jia, *Biomaterials*,  
12 2009, **30**, 6964-6975.
- 13 55. X. Xu, A. K. Jha, R. L. Duncan and X. Jia, *Acta biomaterialia*, 2011, **7**, 3050-3059.
- 14 56. A. K. Jha, R. A. Hule, T. Jiao, S. S. Teller, R. J. Clifton, R. L. Duncan, D. J. Pochan, X.  
15 Jia, C. Ni, X. Li, Z. Chen, H. H. Li, I. Shah and J. Q. Xiao, *Macromolecules*, 2009, **42**,  
16 537-546.
- 17 57. A. K. Jha, M. S. Malik, M. C. Farach-Carson, R. L. Duncan and X. Jia, *Soft matter*, 2010,  
18 **6**, 5045-5055.
- 19 58. A. K. Jha, X. Xu, R. L. Duncan and X. Jia, *Biomaterials*, 2011, **32**, 2466-2478.
- 20 59. S. K. Nigam, *Stem cells translational medicine*, 2013, **2**, 993-1000.
- 21 60. J. S. Harunaga, A. D. Doyle and K. M. Yamada, *Developmental biology*, 2014, **394**, 197-  
22 205.
- 23 61. J. C. Hsu, H. Koo, J. S. Harunaga, K. Matsumoto, A. D. Doyle and K. M. Yamada,  
24 *Developmental dynamics : an official publication of the American Association of*  
25 *Anatomists*, 2013, **242**, 1066-1077.
- 26 62. W. P. Daley, K. M. Gulfo, S. J. Sequeira and M. Larsen, *Developmental biology*, 2009,  
27 **336**, 169-182.
- 28 63. T. Sakai, M. Larsen and K. M. Yamada, *Nature*, 2003, **423**, 876-881.
- 29 64. C. Wei, M. Larsen, M. P. Hoffman and K. M. Yamada, *Tissue engineering*, 2007, **13**,  
30 721-735.
- 31 65. M. Ogawa, M. Oshima, A. Imamura, Y. Sekine, K. Ishida, K. Yamashita, K. Nakajima, M.  
32 Hirayama, T. Tachikawa and T. Tsuji, *Nature communications*, 2013, **4**, 2498.
- 33 66. T. L. Yang, Y. C. Hsiao, S. J. Lin, H. W. Lee, P. J. Lou, J. Y. Ko and T. H. Young,  
34 *Biomaterials*, 2010, **31**, 288-295.
- 35 67. T. L. Yang and T. H. Young, *Biomaterials*, 2008, **29**, 2501-2508.
- 36 68. T. L. Yang and Y. C. Hsiao, *Biomaterials*, 2015, **66**, 29-40.
- 37 69. H. Miyajima, T. Matsumoto, T. Sakai, S. Yamaguchi, S. H. An, M. Abe, S. Wakisaka, K.  
38 Y. Lee, H. Egusa and S. Imazato, *Biomaterials*, 2011, **32**, 6754-6763.
- 39 70. S. B. Peters, D. A. Nelson, H. R. Kwon, M. Koslow, K. A. DeSantis and M. Larsen,  
40 *Matrix biology : journal of the International Society for Matrix Biology*, 2015, **43**, 109-124.
- 41 71. B. J. Baum and S. D. Tran, *Periodontology 2000*, 2006, **41**, 218-223.
- 42 72. D. J. Aframian, R. S. Redman, S. Yamano, J. Nikolovski, E. Cukierman, K. M. Yamada,  
43 M. F. Kriete, W. D. Swaim, D. J. Mooney and B. J. Baum, *Tissue engineering*, 2002, **8**,  
44 649-659.
- 45 73. A. Raza, C. S. Ki and C. C. Lin, *Biomaterials*, 2013, **34**, 5117-5127.
- 46 74. C. Barnes, L. Speroni, K. P. Quinn, M. Montevil, K. Saetzler, G. Bode-Animashaun, G.  
47 McKerr, I. Georgakoudi, C. S. Downes, C. Sonnenschein, C. V. Howard and A. M. Soto,  
48 *PLoS One*, 2014, **9**, e93325.
- 49 75. W. P. Daley, S. B. Peters and M. Larsen, *Journal of cell science*, 2008, **121**, 255-264.
- 50 76. E. S. Radisky and D. C. Radisky, *Journal of mammary gland biology and neoplasia*,  
51 2010, **15**, 201-212.

- 1 77. C. A. DeForest and K. S. Anseth, *Annual review of chemical and biomolecular*  
2 *engineering*, 2012, **3**, 421-444.
- 3 78. X. Du, J. Zhou, J. Shi and B. Xu, *Chemical reviews*, 2015.
- 4 79. M. E. Belowich and J. F. Stoddart, *Chemical Society reviews*, 2012, **41**, 2003-2024.
- 5 80. C. J. Kloxin and C. N. Bowman, *Chemical Society reviews*, 2013, **42**, 7161-7173.
- 6 81. L. Y. Jiang, B. Lv and Y. Luo, *Biomaterials*, 2013, **34**, 2665-2673.
- 7 82. B. W. Han, H. Layman, N. A. Rode, A. Conway, D. V. Schaffer, N. J. Boudreau, W. M.  
8 Jackson and K. E. Healy, *Tissue Eng Part A*, 2015, **21**, 2366-2378.
- 9 83. M. W. Tibbitt and K. S. Anseth, *Science translational medicine*, 2012, **4**, 160ps124.
- 10 84. F. Pampaloni, E. G. Reynaud and E. H. Stelzer, *Nature reviews. Molecular cell biology*,  
11 2007, **8**, 839-845.
- 12 85. S. Sart, A. C. Tsai, Y. Li and T. Ma, *Tissue Eng Part B Rev*, 2014, **20**, 365-380.
- 13 86. E. Fennema, N. Rivron, J. Rouwkema, C. van Blitterswijk and J. de Boer, *Trends in*  
14 *biotechnology*, 2013, **31**, 108-115.
- 15 87. G. Wei and P. X. Ma, *Biomaterials*, 2009, **30**, 6426-6434.
- 16 88. E. S. Place, N. D. Evans and M. M. Stevens, *Nat Mater*, 2009, **8**, 457-470.
- 17 89. S. Pringle, R. Van Os and R. P. Coppes, *Stem cells (Dayton, Ohio)*, 2013, **31**, 613-619.
- 18 90. C. Yoo, J. B. Vines, G. Alexander, K. Murdock, P. Hwang and H. W. Jun, *Biomaterials*  
19 *research*, 2014, **18**, 9.
- 20 91. S. I. Jang, H. L. Ong, A. Gallo, X. Liu, G. Illei and I. Alevizos, *Journal of dental research*,  
21 2015, **94**, 304-311.
- 22 92. S. Wang, E. Cukierman, W. D. Swaim, K. M. Yamada and B. J. Baum, *Biomaterials*,  
23 1999, **20**, 1043-1049.
- 24 93. H. Gray, P. L. Williams and L. H. Bannister, *Gray's Anatomy: The Anatomical Basis of*  
25 *Medicine and Surgery*, Churchill Livingstone, New York, 1995.

26

27

1

2 **Table 1:** Summary of major synthetic materials investigated for salivary gland tissue  
3 engineering.

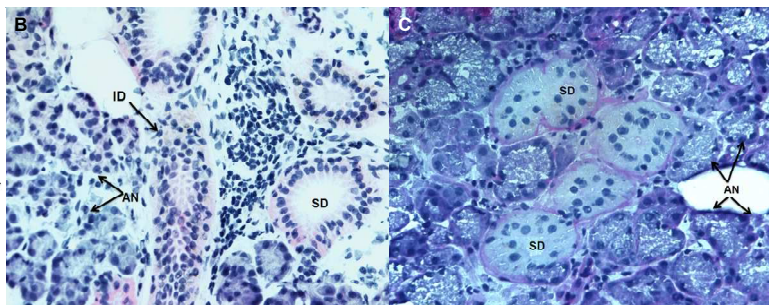
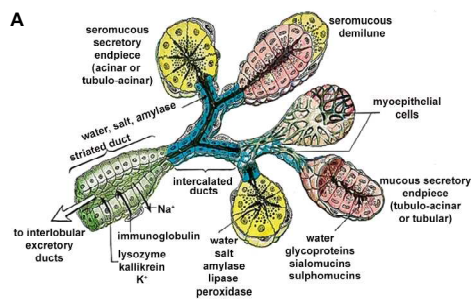


1

Approach	Biomaterials	Cells/tissues	Major observation
2D culture	PLA and PGA (flat disks)	Immortalized human salivary gland cell line (HSG)	Coating of matrix proteins is necessary to support cell attachment and organization. <sup>4, 92</sup>
	PLGA (fibrous scaffolds)	Immortalized adult mouse submandibular gland ductal cell line (SIMS)  Immortalized adult rat parotid gland acinar cell line (ParC10)	More rounded and clustered cell morphology as compared to those grown on planar surfaces; Polarization and the establishment of tight junctions require laminin coating; Additional physical features of the substrate, such as curvature, affects cell polarization and expression of tight junction and water channel proteins. <sup>26-28</sup>
	silk fibroin (porous scaffolds)	Primary salivary gland epithelial cells from rat submandibular gland and parotid gland	Promote epithelial cell growth, facilitate the secretion of matrix proteins and retain the differentiated function. <sup>20</sup>
	HA hydrogels	Primary human salivary gland acinar-like cells from the parotid gland	Acini-like structures with tight junctions, $\alpha$ -amylase expression and an apoptotic central lumen was observed on HA gels with an elastic modulus of 2000 Pa and incorporating PInDIV peptide. <sup>23</sup>
	[PEG(RGD)-C12] <sub>n</sub>	Human primary salivary gland myoepithelial cells	Provide guidance cues for the attachment and elongation of myoepithelial cells. <sup>31</sup>
3D culture	PEG hydrogels	A mixture of primary acinar and ductal cells from mouse submandibular gland	Cells survive the encapsulation in the thiol-ene network, but remain as single cells without forming organized acini-like structures; Encapsulation of pre-assembled spheroids improved viability, promoted cell proliferation, and established and preserved cell-cell contacts. <sup>41</sup>
	HA/PEG hydrogels	Primary human salivary gland acinar-like cells from the parotid gland	Cells self-assembled into acini-like structures ~50 $\mu$ m in size; the structures demonstrated neurotransmitter-stimulated protein secretion and fluid production; Incorporation of PInDIV peptide in the hydrogel induced lumen formation. <sup>15, 23, 37</sup>
ex vivo culture of embryonic tissues	PLGA fibrous scaffold; PVDF or chitosan membrane	Mouse embryonic submandibular glands	Support the branching morphogenesis if embryonic salivary gland <sup>69 16</sup>
	Alginate or polyacrylamide gels	Mouse embryonic submandibular glands	Surface immobilization of cell adhesive peptide or protein is necessary; Softer gels enhance the bud expansion and cleft formation, whereas stiffer gels attenuate them; Partial rescue of acini structure and differentiation can be achieved by adding exogenous growth factors or by transferring glands from stiff to soft substrates.

2 **Figures:**

1 **Figure 1:** Structure and organization of the human salivary gland. (A): Schematic illustration of  
2 the cross-sectional view of the salivary gland composed of the serous acinus and the  
3 intercalated duct (adapted from Gray et al, 1995<sup>93</sup> with permission). (B): Hematoxylin and eosin  
4 staining of human salivary gland tissue (20x). (C): Periodic acid Schiff staining of the salivary  
5 gland tissue (40x). Arrows point to AN, acini; AC, acinar cells; ID, intercalated duct; SD, striated  
6 ducts; and DC, ductal cells.

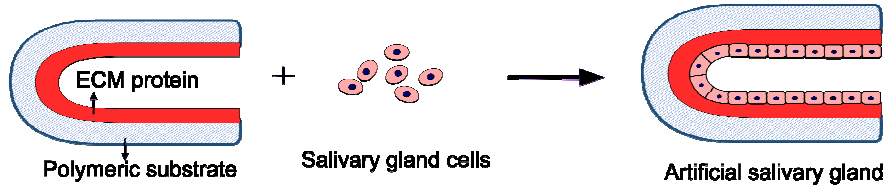


7  
8

1  
2  
3  
4  
5

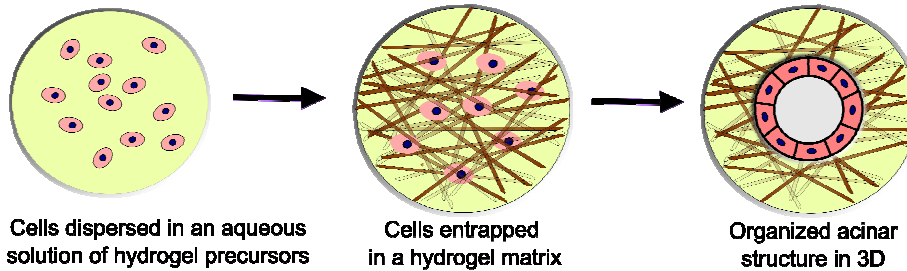
**Figure 2.** Biomaterials based strategies for salivary gland tissue regeneration. **(A):** 2D culture of salivary gland cells on a blind-end, polymeric tubular device; **(B):** 3D culture of salivary gland cells in an instructive and permissive hydrogel matrix; **(C):** *ex vivo* culture of embryonic tissues on a compliant substrate.

**A: 2D culture on a blind-end tubular device**



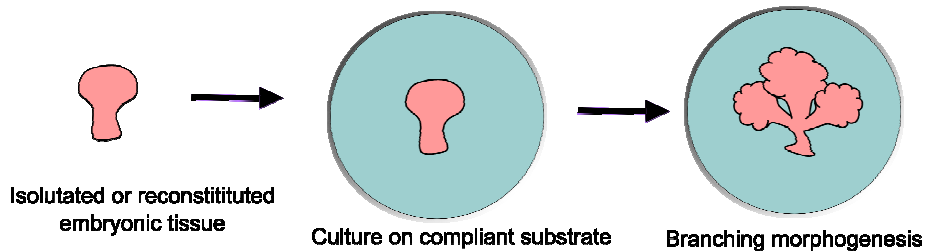
- a. Substrate topography, porosity, elasticity and biocompatibility; b. ECM signals;  
c. Non-secretory functions of ductal cells. d. Uncertainties of genetic manipulations.

**B: 3D culture in a permissive hydrogel matrix**



- a. Crosslinking chemistry, network connectivity; b. Cell-instructive signals;  
c. Matrix elasticity, degradability and reversibility;  
d. Establishment of acini-like structures with close cell-cell contact and proper polarization;  
e. Methods for connecting individual acini and for producing branched constructs.

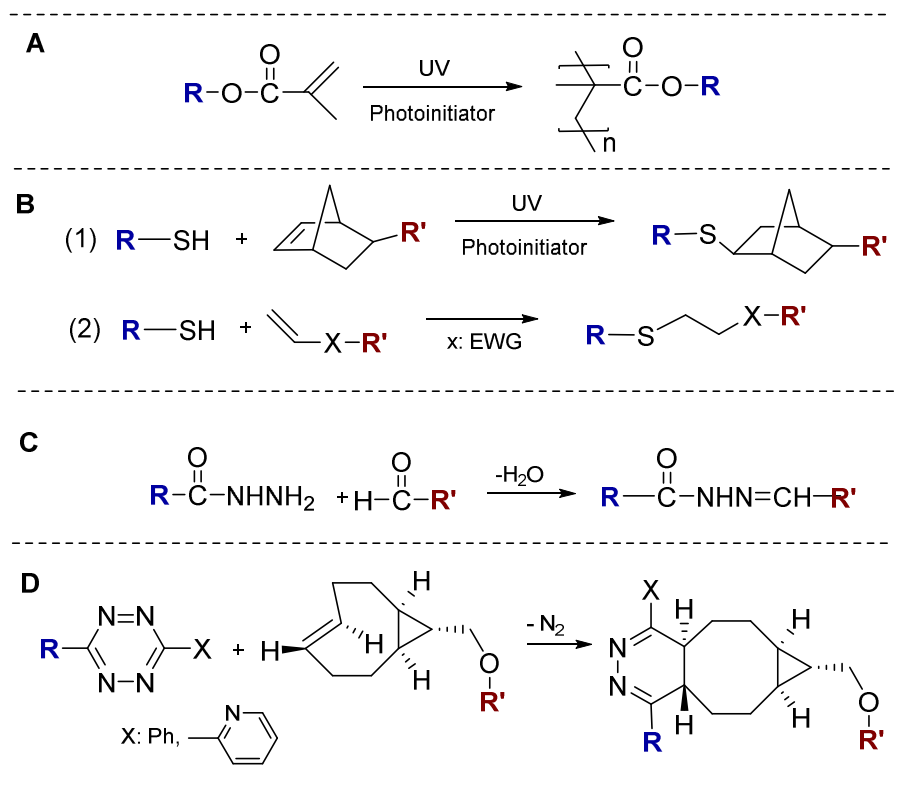
**C: *ex vivo* culture of embryonic cells/tissues**



- a. Regenerative potential of embryonic tissues;  
b. Substrate stiffness, porosity and the presentation of biological signals.

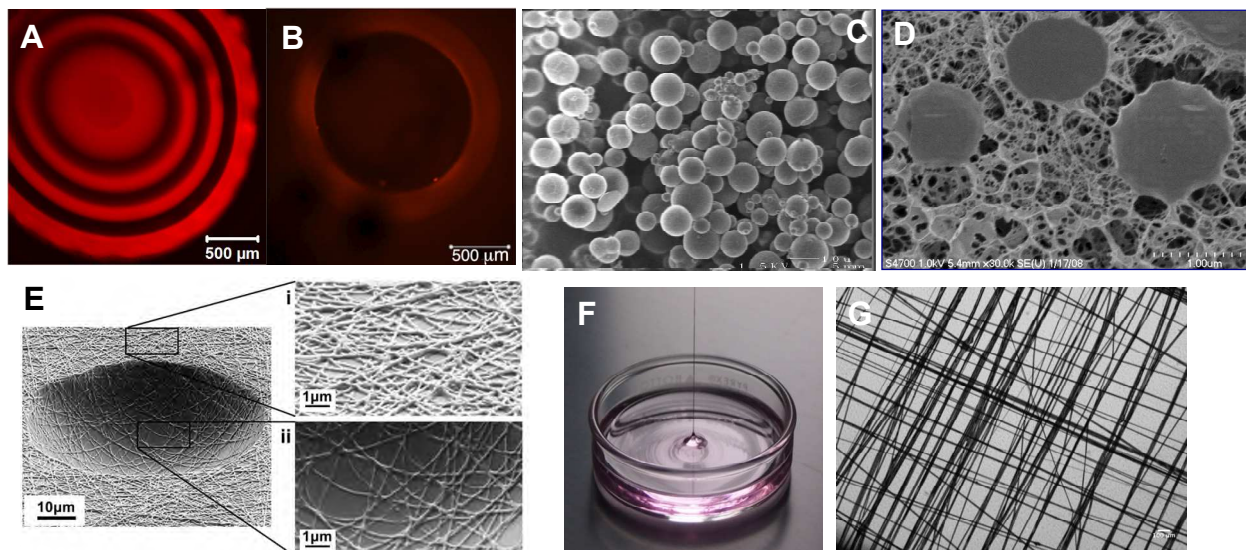
6  
7

1  
 2 **Figure 3.** Chemistries applied to the synthesis of biomaterials targeting salivary gland tissue  
 3 engineering applications. **(A):** Radical-mediated chain polymerization; **(B):** Thiol-ene photo-  
 4 polymerization (1) and Michael addition (2); **(C):** Hydrazone ligation; **(D):** Inverse electron  
 5 demand Diels-Alder reaction. R and R': PEG, HA, peptide or an alkyl chain.



1  
2  
3  
4  
5  
6  
7  
8  
9  
10  
11  
12  
13  
14

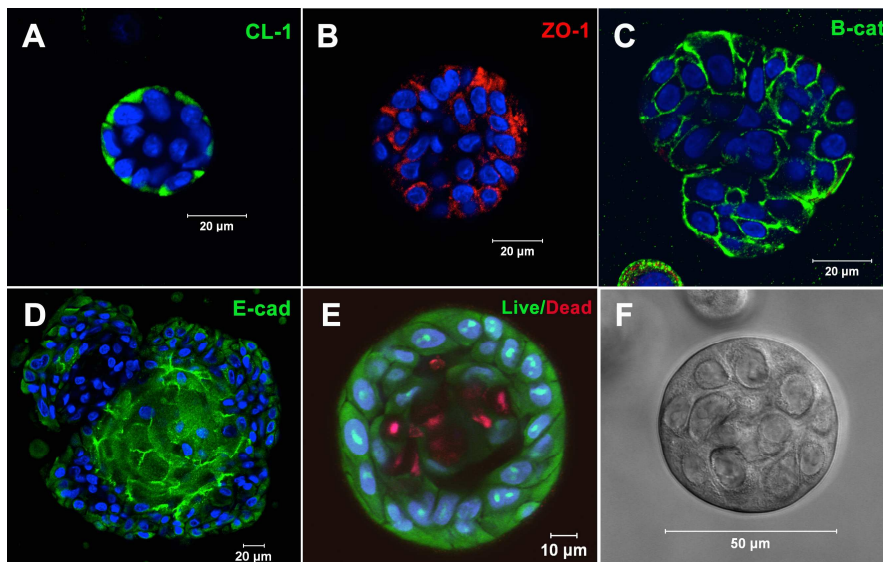
**Figure 4.** Representative microscopy images of biomaterials developed for salivary gland tissue engineering. **(A):** Confocal microscopy image of the central slice of a HA-based solid hydrogel sphere spatially tagged TCO-modified Alexa Fluor® 647 (red). Black regions correspond to crosslinked HA gel layer without the dye. **(B):** A z-stack confocal image showing the top view of the HA hydrogel channel covalently labeled with Alexa Fluor® 647 (red). Black region inside the red wall corresponds to a water-filled channel interior. **(C):** Scanning electron micrograph (SEM) of HA-based HGP. **(D):** Cryogenic SEM image of HA-based doubly crosslinked networks. **(E):** SEM image of PLGA nanofibrous crater created by electrospinning and photolithography. **(F):** Digital picture showing a multiblock copolymer fiber pulled out of the oil/water interface during the interfacial bioorthogonal polymerization process. **(G):** Crosshatched multiblock copolymer mesh imaged under light microscope. Reprinted with permission from Zhang et al, 2014 (A-B),<sup>51</sup> Jia et al, 2006 (C),<sup>52</sup> Jha et al, 2009 (D),<sup>56</sup> and Soscia et al, 2013 (E)<sup>28</sup> and Liu et al, 2015 (F-G).<sup>31</sup>



1

2 **Figure 5:** Acini-like spheroids in 3D HA hydrogels. Spheroid structures express tight junction  
3 markers CL-1 (**A**), ZO-1 (**B**), E-cadherin (**D**) and adherens junction marker,  $\beta$ -catenin (**C**). (**E**):  
4 Live/Dead staining of Syto13 positive green cells and propidium iodide positive red cells. Nuclei  
5 stain blue. (**F**): Representative phase image of an acinus-like structure. Reprinted from  
6 Pradhan-Bhatt et al, 2013<sup>15</sup> with permission.

7

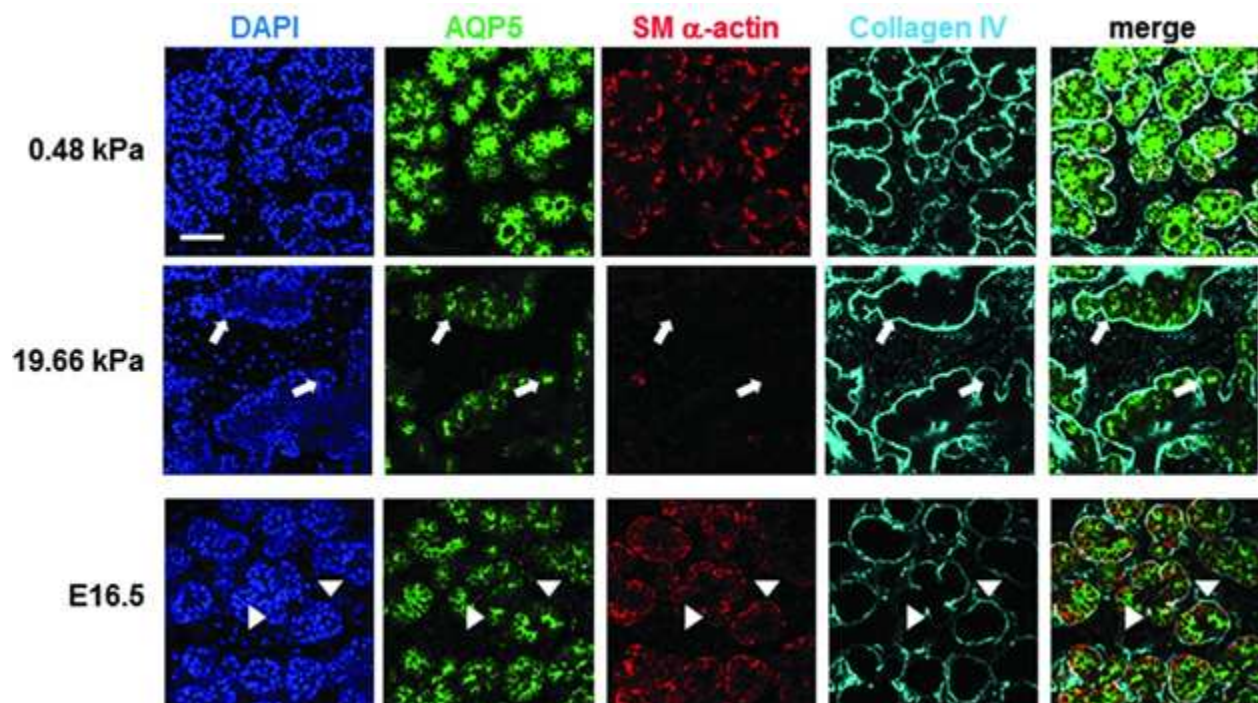


8

9



1  
2 **Figure 6.** Effect of substrate stiffness on the morphology and cell arrangement of ex vivo  
3 cultured embryonic gland. Representative confocal images were captured from the center of  
4 organ explants. Collagen IV (cyan) delineates the boundary of the rounded buds, SM  $\alpha$ -actin  
5 (red) indicates the location of the myoepithelial cells and AQP5 (green) stains for the  
6 proacinar/acinar cells. Compared to those cells cultured on a more compliant (0.48 kPa)  
7 substrate and the glands developed *in vivo* (embryonic day 16.5, E16.5), explants cultured on  
8 stiff (19.66 kPa) substrates exhibit inconsistent, less organized gland morphology, less  
9 homogeneous bud structures, decreased expression of AQP5 and SM  $\alpha$ -actin, and aberrant  
10 acinar structures lacking SM  $\alpha$ -actin-positive cells (white arrows). In the gland grown *in vivo*,  
11 AQP5 is localized apically with the inner epithelial cells (green), highlighted by arrow heads, SM  
12  $\alpha$ -actin (red) is expressed in the outer cuboidal cells of the proacinar structures, interior to the  
13 basement membrane, as detected by anti-Col IV antibody (cyan). Scale bar=50  $\mu$ m.<sup>16</sup>

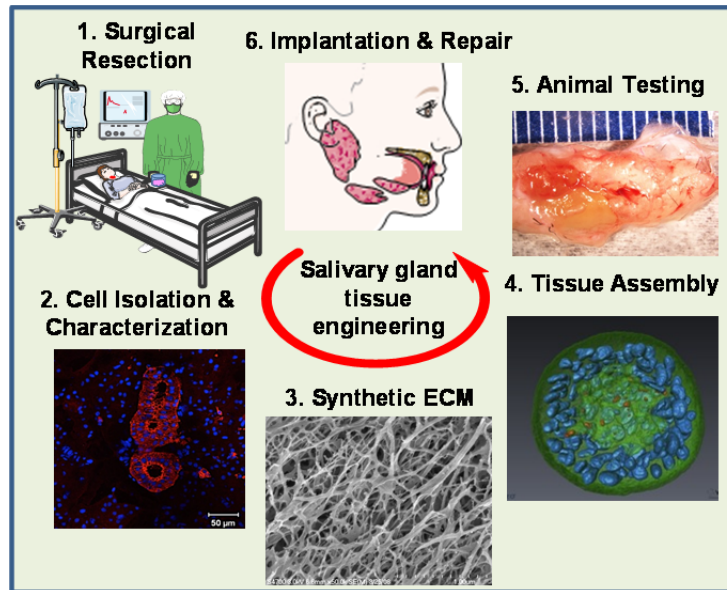


14  
15  
16

1



1 Table of Content (TOC) Graphic



- 2
- 3
- 4